Saxena, V. P., & Wetlaufer, D. B. (1970) *Biochemistry 9*, 5015-5023.
Schaffer, S. W., Ahmed, A. K., & Wetlaufer, D. B. (1975) *J. Biol. Chem. 250*, 8483-8486.
Scheraga, H. A., Konishi, Y., & Ooi, T. (1984) *Adv. Biophys. 18*, 21-41.
Scheraga, H. A., Konishi, Y., Rothwarf, D. M., & Mui, P. W. (1987) *Proc. Natl. Acad. Sci. U.S.A. 84*, 5740-5744.
Schmid, F. X. (1986) *Methods Enzymol. 131*, 70-82.
Tang, J.-G., Wang, C.-C., & Tsou, C.-L. (1988) *Biochem. J. 255*, 451-455.
Thornton, J. M. (1981) *J. Mol. Biol. 151*, 261-287.
Udgaonkar, J. B., & Baldwin, R. L. (1988) *Nature 335*, 694-699.
Varandani, P. T., Nafz, M. A., & Chandler, M. L. (1975) *Biochemistry 14*, 2115-2120.
Wearne, S. J., & Creighton, T. E. (1988) *Proteins 4*, 251-261.
Wetlaufer, D. B., Branca, P. A., & Chen, G.-X. (1987) *Protein Eng. 1*, 141-146.
Wetterau, J. R., Combs, K. A., Spinner, S. N., & Joiner, B. J. (1990) *J. Biol. Chem. 265*, 9800-9807.
Yamauchi, K., Yamamoto, T., Hayashi, H., Koya, S., Takikawa, H., Toyoshima, K., & Horiuchi, R. (1987) *Biochem. Biophys. Res. Commun. 146*, 1485-1492.

Catalysis of the Oxidative Folding of Ribonuclease A by Protein Disulfide Isomerase: Pre-Steady-State Kinetics and the Utilization of the Oxidizing Equivalents of the Isomerase†

Michelle M. Lyles and Hiram F. Gilbert*
Verna and Marrs McLean Department of Biochemistry, Baylor College of Medicine, Houston, Texas 77030
Received May 4, 1990; Revised Manuscript Received September 26, 1990

ABSTRACT: At low concentrations of a glutathione redox buffer, the protein disulfide isomerase (PDI) catalyzed oxidative renaturation of reduced ribonuclease A exhibits a rapid but incomplete activation of ribonuclease, which precedes the steady-state reaction. This behavior can be attributed to a GSSG-dependent partitioning of the substrate, reduced ribonuclease, between two classes of thiol/disulfide redox forms, those that can be converted to active ribonuclease at low concentrations of GSH and those that cannot. With catalytic concentrations of PDI and near stoichiometric concentrations of glutathione disulfide, approximately 4 equiv (2 equiv of ribonuclease disulfide) of GSH are formed very rapdily followed by a slower formation of GSH, which corresponds to an additional 2 disulfide bond equiv. The rapid formation of RNase disulfide bonds and the subsequent rearrangement of incorrect disulfide isomers to active RNase are both catalyzed by PDI. In the absence of GSSG or other oxidants, disulfide bond equivalents of PDI can be used to form disulfide bonds in RNase in a stoichiometric reaction. In the absence of a glutathione redox buffer, the rate of reduced ribonuclease regeneration increases markedly with increasing PDI concentrations below the equivalence point; however, PDI in excess over stoichiometric concentrations inhibits RNase regeneration.

The formation of disulfide bonds in extracellular, eukaryotic proteins requires both a source of oxidizing equivalents and a catalyst for the process. Cysteine-containing proteins are synthesized and cotranslationally inserted into the lumen of the endoplasmic reticulum in the reduced (SH) form. Disulfide bond formation occurs during or soon after translation, significantly preceding the appearance of the mature protein at the cell surface (Bergman & Kuehl, 1979; Peters & Davidson, 1982). Disulfide bond formation and rearrangement in in vitro oxidative folding systems is significantly slower than the in vivo process, so the need for some in vivo catalyst has been recognized for some time (Goldberger et al., 1963).

Protein disulfide isomerase (PDI),[1] an abundant protein of the endoplasmic reticulum, catalyses the oxidative folding of proteins in vitro (Lambert & Freedman, 1985) and most likely in vivo (Bulleid & Freedman, 1988). In vitro, oxidizing equivalents may be provided by a variety of disulfides (Hillson et al., 1984; Morin & Dixon, 1985; Varandani et al., 1975), but in vivo, the source of oxidizing equivalents is unknown. The enzyme was initially isolated by its ability to catalyze the oxidative renaturation of proteins that contain disulfide bonds (Goldberger et al., 1963). PDI has been implicated in the oxidative folding process although recently a number of other, very diverse functions have been suggested for the protein (Cheng et al., 1987; Obata et al., 1988; Koivu et al., 1987; Geetha-Habib et al., 1988; Wetterau et al., 1990).

In a glutathione redox buffer, PDI functions catalytically—multiple turnovers regenerate native RNase from the reduced form at the expense of oxidizing equivalents from GSSG (Lyles & Gilbert, 1991). However, PDI is a very abundant protein (Hillson & Freedman, 1984). If the enzyme were uniformly distributed in the cell, the intracellular concentration would be about 20 μM (Lyles & Gilbert, 1991), comparable to the total cellular concentration of glutathione disulfide (Gilbert, 1990). The local concentration of PDI in the lumen of the endoplasmic reticulum would, naturally, have to be much higher, likely approaching the millimolar range. Because of its potentially high, local concentration in vivo, the

† This work was supported by NIH Grant GM-40379.

[1] Abbreviations: PDI, protein disulfide isomerase; RNase, bovine pancreatic ribonuclease A; GSH, glutathione; GSSG, glutathione disulfide; DTT, dithiothreitol; cCMP, cytidine 2',3'-cyclic monophosphate.

0006-2960/91/0430-619$02.50/0

stoichiometric reaction of reduced proteins with PDI should be considered. The experiments reported here reveal that stoichiometric concentrations of PDI not only catalyze the oxidative folding of RNase but can also directly provide oxidizing equivalents for the process by utilizing its disulfide bonds as oxidizing agents. While this does not solve the problem of supplying net oxidizing equivalents to the lumen of the endoplasmic reticulum, it does raise the possibility that, in addition to its function as a catalyst, PDI may provide substantial redox buffering capacity.

Experimental Procedures

Materials and Methods. The source of materials and the general methodology employed have been previously described (Lyles & Gilbert, 1991).

Formation of GSH during the Reaction of RNase with GSSG. Incubations of RNase with 0.1 mM GSSG were initiated by the addition of fully reduced RNase (8.5 μM) to a solution of PDI (1.4 μM) containing 0.1 mM GSSG in 0.1 M Tris–acetate and 2 mM EDTA, pH 8.0, 25.0 °C. A parallel reaction containing no PDI was also performed under the same conditions. At various times, aliquots were removed and diluted into 1 M HCl and frozen in liquid nitrogen to stop the reaction. The GSH in the quenched samples was measured by the HPLC method of Alpert and Gilbert (1985). Parallel samples of the same composition were continuously assayed for RNase activity. In the absence of PDI and RNase, no detectable GSH formation was observed.

Stoichiometric Oxidation of RNase by PDI. RNase (4.1–6.3 μM) was added to a cuvette containing various concentrations of PDI in 0.1 M Tris–acetate, pH 8.0, 2 mM EDTA, 25.0 °C, and 4.3 mM cCMP. The activity of RNase was followed continuously as previously described (Lyles & Gilbert, 1991). The extent of RNase activation was determined from the amount of RNase activity observed after the initially rapid activation of RNase had stopped. The velocity of the reaction was determined immediately following a short (1–3 min) lag in the formation of active RNase. The effect of oxygen on the amount of RNase formed on incubation with PDI was also determined by incubating PDI and RNase in argon-degassed buffer and maintaining the samples under an atmosphere of humidified argon. RNase activity was determined at approximately 60, 120, and 180 min after mixing by withdrawing aliquots and assaying for RNase activity at pH 5.0 by using a spectrophotometric assay for cCMP hydrolysis. The change in RNase activity between the 120 and 180 min time points was <20% for PDI concentrations greater than 2 μM.

Titration of free cysteine in PDI in the presence of 6 M Gdn·HCl (pH 7.5) with Ellman's reagent (Ellman, 1959) showed 1.2 ± 0.1 equiv of free cysteine per mole of PDI (55 130 kDa) (Yamauchi et al., 1987), and the stoichiometry of reduction of this preparation of PDI by GSH (Gilbert, 1989) showed three sequential reduction processes with a total disulfide bond content of 2.2–2.3 mol/mol of PDI. PDI concentrations were routinely determined by the absorbance at 280 nm ($E_{0.1\%}$ = 1.1), which was determined by quantitative amino acid composition measurements.

Results

Pre-Steady-State Formation of Active RNase. Under very specific redox conditions (low GSSG and low GSH), the first few minutes of the PDI-catalyzed oxidative folding of reduced RNase reveal kinetically complex behavior. After a shoft lag, the establishment of the steady-state velocity (Lyles & Gilbert, 1991) is preceeded by a rapid (1–4 min) phase of active RNase

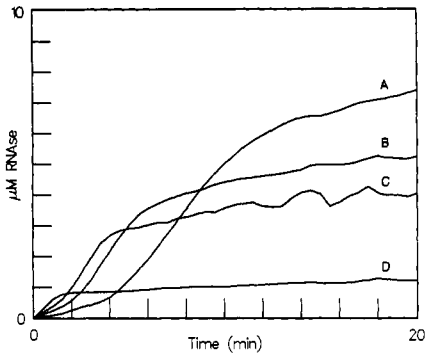

FIGURE 1: GSSG dependence of active RNase formation observed in the PDI-catalyzed, oxidative folding of reduced RNase A. All reactions were performed at pH 8.0 (0.1 M Tris–acetate, 2 mM EDTA), 25.0 °C. Reactions were initiated by adding fully reduced RNase A (8.4 μM final concentration) to solutions containing PDI (1.4 μM) and different concentrations of GSSG. No GSH was added to the reaction mixtures. The concentration of active RNase was determined continuously as previously described (Lyles & Gilbert, 1991). Initial GSSG concentrations were: A, 0.1 mM; B, 0.2 mM; C, 0.5 mM; D, 1.0 mM.

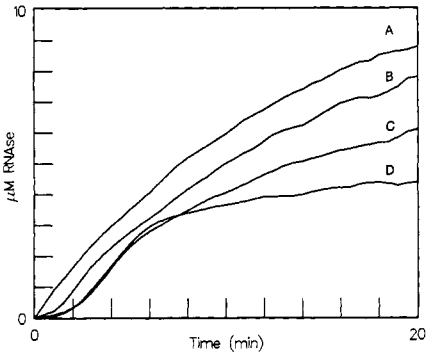

FIGURE 2: Effect of GSH concentration on the rapid phase of RNase formation observed in the PDI-catalyzed, oxidative folding of reduced RNase A. All reactions were performed at pH 8.0 (0.1 M Tris–acetate, 2 mM EDTA), 25.0 °C. Reactions were initiated by adding fully reduced RNase A (8.4 μM final concentration) to solutions containing PDI (1.4 μM) and 0.2 mM GSSG. The concentration of active RNase was determined continuously as previously described (Lyles & Gilbert, 1991). The initial GSH concentrations were (A) 1.0 mM, (B) 0.5 mM, (C) 0.1 mM, and (D) 0.05 mM.

formation after which the reaction slows to a lower steady-state velocity (Figures 1 and 2). The amount of active RNase formed in this rapid phase is significantly less than that expected from complete activation of the RNase (8.4 μM), although sufficient GSSG is present to activate all of the added RNase. The amount of RNase activity recovered in the rapid phase of the reaction does not correspond to that expected from stoichiometric turnover of PDI (0.93 μM RNase). In the absence of GSSG, there is no significant activation of RNase above the small amount expected from stoichiometric turnover of PDI (see below), and in the absence of both PDI and GSSG there is no substantial increase in RNase activity during the 30–60-min assay, suggesting that oxygen-dependent activation of RNase does not provide a significant source of oxidizing equivalents under these conditions.

The concentration of GSSG affects the amount of active RNase formed during this rapid phase of the reaction. At low concentrations of GSSG (0.05–0.2 mM), virtually all of the RNase present is eventually converted to active enzyme (8.4 μM) (Figure 1, curve A), but at higher GSSG concentrations, the amount of active RNase formed in the rapid phase declines sharply (Figure 1, curves B–D). At lower GSSG concentrations, the burst is preceded by a short lag. The length of the lag, in turn, decreases with increasing GSSG concentration

(Figure 1). While the lag and extent of the rapid RNase activation are GSSG-dependent, the actual velocity of RNase activation during the burst is virtually independent of the GSSG concentration.

At a concentration of 8.3 μM RNase, the stoichiometric conversion of reduced RNase to the native enzyme by GSSG would yield, at most, 66 μM GSH (eq 1). Additional GSH

$$RNase(SH)_8 + 4GSSG \rightarrow RNase(SS)_4 + 8GSH \quad (1)$$

present during the reaction does not substantially affect the velocity of the fast activation phase (Figure 2); however, an increased GSH concentration increases the velocity of the steady-state reaction following the rapid phase and makes all of the RNase available for oxidative folding so that full RNase activity is regained. In the presence of added GSH, the rapid pre-steady-state phase disappears not because the rate of this phase declines but because RNase activation continues at near the same rate until all of the RNase has been converted to active enzyme.

At higher GSSG concentrations, the decrease in the amount of RNase formed during the rapid phase could result from either PDI inactivation or from a GSSG-dependent partitioning of reduced RNase into nonnative redox isomers (Creighton, 1978; Konishi et al., 1982) that cannot be converted to active RNase at the low GSH concentration present during the assay. After completion of the rapid phase of the reaction in the presence of 0.5 mM GSSG, the reaction essentially stops when only 60% of the RNase has been converted to the active form (Figure 3A, curve 1). The addition of fresh PDI at this point (Figure 3A, curve 2) does not result in activation of additional RNase. Thus, the inability to completely activate all of the RNase is not the result of a time-dependent PDI inactivation during the assay. In contrast, adding an additional aliquot of reduced RNase results in an activation of the added RNase that is virtually identical with that initially observed (Figure 3B, curve 2). The inability to completely renature RNase under these conditions does not arise from the effects of proline isomerization (Lang & Schmid, 1988), since full RNase activity can be recovered by adding GSH (1 mM) after a 30-min incubation of RNase with PDI and GSSG (4 mM) (data not shown).

The redox isomer or isomers of RNase that are competent substrates for PDI are formed only slowly in the absence of PDI. Incubation of RNase with 0.5 mM GSSG in the absence of PDI for 10 min followed by the addition of PDI results in the same lag and burst that was observed when PDI was added initially (Figure 3C).

Formation of GSH. At intermediate GSSG concentrations (0.05–0.1 mM), added GSH is not required to maintain the steady-state velocity, and RNase activation proceeds to completion. Since oxygen-dependent processes do not contribute significantluy to disulfide bond formation under these conditions, this provides the opportunity to follow the thiol/disulfide exchange between RNase and GSSG by measuring the stoichiometric formation of GSH during the GSSG-dependent oxidation of reduced RNase. The formation of either an intramolecular disulfide or glutathione mixed disulfide in RNase results in the formation of 1 equiv of GSH per RNase thiol that is converted to the disulfide form (eqs 2 and 3).

$$RNase(SH)_2 + GSSG \rightleftharpoons RNase(SS) + 2GSH \quad (2)$$

$$RNase(SH) + GSSG \rightleftharpoons RNase(SSG) + GSH \quad (3)$$

With a reduced RNase concentration of 8.3 μM, 33 μM GSSG is required stoichiometrically to form the four disulfide bonds found in native RNase and 66 μM GSH would be

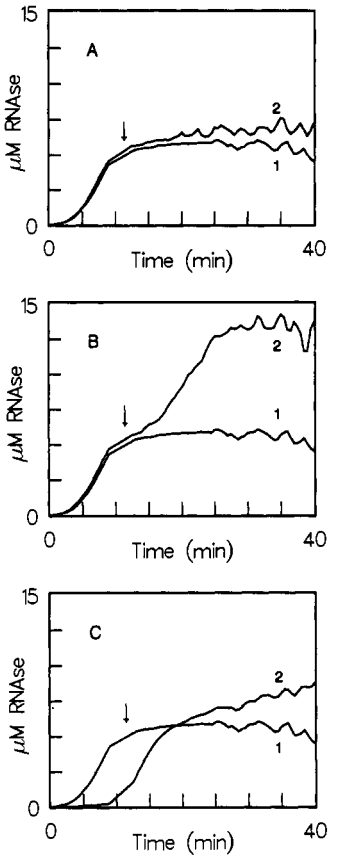

FIGURE 3: Effects of the addition of PDI or RNase after the rapid phase of RNase activation on the oxidative renaturation of reduced RNase. All reactions were performed at pH 8.0 (0.1 M Tris–acetate, 2 mM EDTA), 25.0 °C, and were initiated at time zero by the addition of 8.5 μM fully reduced RNase to a solution containing 1.4 μM PDI and 0.5 mM GSSG. Further additions were made as indicated at the arrow. In all panels, curve 1 shows the effect of adding only buffer at the arrow. (A) Curve 2 is observed after adding additional PDI (1.4 μM) at the arrow. (B) Curve 2 is observed after adding additional RNase (8.5 μM) at the arrow. (C) Curve 2 is observed after adding PDI (1.4 μM) at the arrow to an assay that initially included 8.5 μM RNase and 0.5 mM GSSG but did not include PDI.

formed. RNase oxidation and activity were examined by folding reduced RNase in the absence of added GSH, where the stoichiometric evolution of GSH from GSSG (0.1 mM) was monitored as a function time. Figure 4 confirms that, under these conditions, disulfide bond formation (evidenced by the generation of GSH) is significantly faster than the regain of ribonuclease activity (Givol et al., 1964).

Both the catalyzed and uncatalyzed reactions quickly (<1 min) generate GSH concentrations equivalent to the formation of two intramolecular (or four intermolecular) disulfide bonds corresponding to 50% of the total GSH evolved during the total reaction (Figure 4). This rapid disulfide formation occurs without significant RNase activation (Figure 4). The uncatalyzed reaction slowly generates more oxidized RNase species (evidenced by further GSH release). On the other hand, the PDI-catalyzed yields more highly oxidized RNase species rather quickly (5 min). The total equivalents of GSH formed per RNase upon completion of the PDI-catalyzed reaction is 7.8, very close the theoretical value of 8 for complete reaction, suggesting that almost all of the cysteine residue of RNase are present as intramolecular or intermolecular disulfides even in the early stages of the PDI-catalyzed reaction. For both the catalyzed and uncatalyzed reactions, the formation of disulfide bonds is significantly faster than the generation of enzyme activity, consistent with previous observations for the

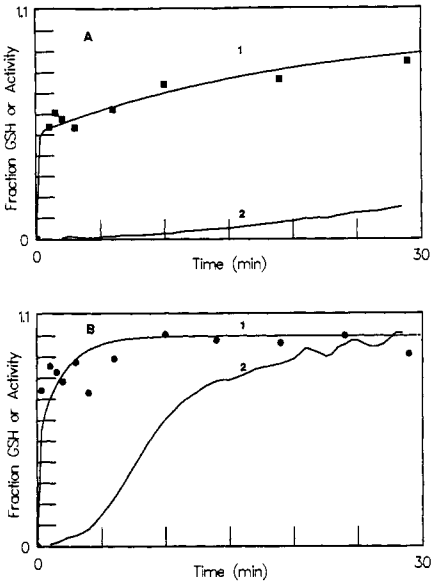

FIGURE 4: GSH formation and oxidative activation of RNase resulting from the reaction of fully reduced RNase with GSSG. Fully reduced RNase A (8.4 μM final concentration) was added to a solution containing 0.1 mM GSSG and 1.4 μM PDI (pH 8.0, 0.1 M Tris-acetate, 2 mM EDTA). The formation of GSH as a function of time was determined by HPLC (Alpert & Gilbert, 1985). The activity of RNase was followed in a parallel, continuous assay. Results are shown as the fraction of the expected stoichiometric production of GSH or as the fraction of expected active RNase A. The total amount of GSH formed (fraction = 1.0) was 66 μM. Fully active RNase (fraction = 1.0) corresponds to a concentration of 8.5 μM (A) Reaction in the absence of PDI; (■) GSH formed. Curve 2 is the fraction of active RNase measured in a parallel continuous assay under the same conditions. (B) Reaction in the presence of PDI; (●) GSH formed. Curve 2 is the fraction of active RNase measured in a parallel continuous assay under the same conditions.

uncatalyzed reaction (Hantgan et al., 1974; Konishi et al., 1981; Wearne & Creighton, 1988). After the burst of 2 disulfide bond equiv of GSH, the rate of the PDI-catalyzed formation of GSH is significantly faster than the uncatalyzed oxidation, showing that PDI, in fact, catalyzes the net GSSG-dependent oxidation of RNase as well as subsequent rearrangements to the active form.

Stoichiometric Activation of RNase by PDI. In the absence of GSSG, the oxidizing equivalents necessary for the oxidative refolding of reduced, inactive RNase can be provided by PDI itself. The PDI added to initiate the oxidative folding of fully reduced RNase contains 2.2–2.3 disulfides/mol whereas RNase oxidation requires 4 disulfide equiv/mol of RNase. At substoichiometric PDI concentrations, only a fraction of the total RNase is converted to the active enzyme. The extent of RNase activation as a function of the molar ratio of [PDI]/[RNase] (Figure 5) in four independent experiments demonstrates that increasing concentrations of PDI activate increasing quantities of RNase until the concentration of disulfides provided by PDI equals the concentration of disulfide bonds to be formed in RNase. At the equivalence point, 1.5 ± 0.2 mol of PDI are required to regenerate 1 mol of RNase, indicating that 2.6 ± 0.3 disulfide bond equiv is derived from each mole of PDI. Results obtained in argon-degassed buffer by using a discontinuous assay for the extent of RNase activation are comparable to those obtained by employing the continuous assay for RNase renaturation, suggesting a minimal contribution of oxygen to the formation of disulfides in RNase (Figure 5).

The preparations of PDI used in these experiments contained between 1.1–1.3 mol/mol of free cysteine residues and 2.2–2.3 mol of GSH-reducible disulfides/mol of PDI. The disulfides

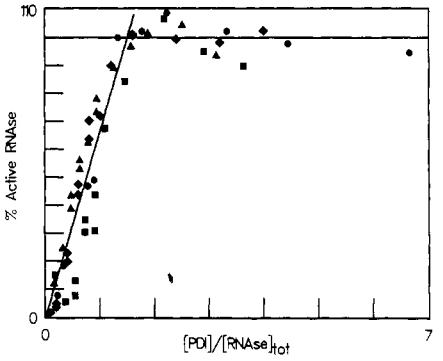

FIGURE 5: Dependence of the total amount of active RNase formation on the ratio of PDI to total RNase concentration in the absence of a redox buffer. All reactions were performed at pH 8.0 (0.1 M Tris-acetate chloride, 2 mM EDTA), 25.0 °C. RNase was added to reaction mixtures containing different concentrations of PDI. The vertical axis represents the maximum concentration of active RNase observed after the formation of active RNase had ceased: (●) 4.1 μM RNase; (◆) 6.4 μM RNase; (■) 5.5 μM RNase; (▲) 5.0 μM RNase monitored by a discontinuous assay. The equivalence point is shown at a ratio of PDI to RNase of 1.5 ± 0.2.

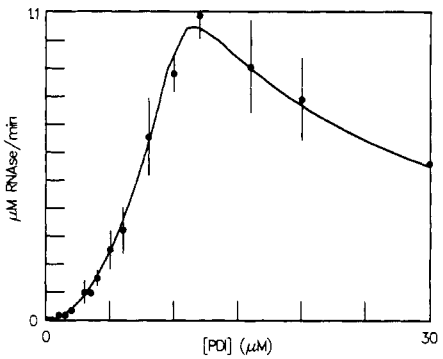

FIGURE 6: Dependence of the rate of the PDI-catalyzed oxidative folding of reduced RNase in the absence of a redox buffer on the concentration of PDI. All reactions were performed at pH 8.0 (0.1 M Tris-acetate chloride, 2 mM EDTA). Fully reduced RNase A (4.1–6.3 μM final concentration) was added to solutions containing various concentration of PDI. PDI served as the sole source of oxidizing equivalents in the reaction. After a short lag (1.3 min), the initial velocity of the formation of active RNase was measured. The average velocities from three independent determinations are shown. The error bars indicate the standard deviation.

in the preparation of PDI used in this study also clearly displayed triphasic kinetics of reduction by GSH (Gilbert, 1989), indicating the presence of three types of disulfide bonds in PDI. The observed rate constants for each of the three phases of the reduction were comparable (±15%) to the previously reported values (data not shown) (Gilbert, 1989). The presence of free cysteine residues in PDI under denaturing conditions has been reported previously (Carmichael et al., 1979) and suggests that at least two of the cysteines are present in both the thiol and disulfide forms. The disulfides are not intermolecular. Non-reducing SDS gels of the alkylated protein showed <5% dimeric PDI (data not shown).

Under conditions where the oxidizing equivalents for RNase activation are provided solely by the disulfide bonds initially present in PDI, the rate of RNase activation is a complex function of the concentration of PDI. At sub-stochiometric PDI concentrations, the rate is greater than first order in PDI concentration (Figure 6), but concentrations of PDI exceeding the equivalence point decrease the rate of RNase refolding.

Discussion

Rapid Activation of RNase. Under specific conditions (low GSH and low GSSG), the PDI-catalyzed oxidative renatu-

Scheme I: Mechanism for the Initial Formation of Active RNase from the Reduced Protein at Low GSSG and GSH Concentrations in the Presence of PDI

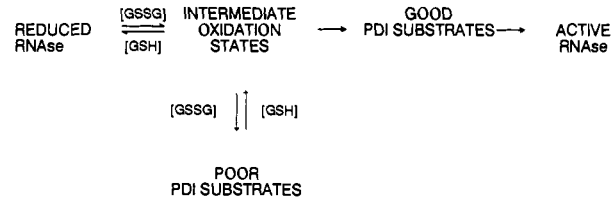

ration of reduced RNase exhibits a rapid phase of RNase activation, which precedes the slower, steady-state velocity. The results are consistent with a kinetic model in which the initially reduced RNase rapidly partitions into two kinetically different popoulations of redox isomers—a population that can be converted to native, active RNase with the low concentrations of GSH present during the assay and a population that cannot (Scheme I). At the low GSH and GSSG concentrations where these effects are observed, reversible interconversion of RNase redox isomers (equilibrium) would lead to complete conversion of all of the added RNase to the active enzyme rather than the partial activation that is observed.

The rapid phase of RNase formation is preceded by a lag, comparable to the lag that precedes the steady-state reaction at higher glutathione concentrations (Lyles & Gilbert, 1991). The lag time decreases significantly with increasing GSSG concentration (Figure 1) and with increasing GSH concentration (Figure 2), suggesting that the formation of the intermediate(s) preceding the rate-limiting step of the PDI-catalyzed reaction is accelerated by both GSSG and GSH—consistent with the first step shown as an approach to equilibrium in the mechanisms of Scheme I.

Although it decreases the lag time, increasing the concentration of GSSG significantly decreases the total amount of RNase that is activated during the fast phase (Figure 1). If the formation of both productive and nonproductive intermediates were dependent on GSSG with the same kinetic order, the partitioning between the two pathways would be fixed by the relative rate constants and would be independent of the GSSG concentration.

On the other hand, increasing the GSH concentration, even in the presence of GSSG, rescues misoxidized RNase species that are not good PDI substrates and converts them to species that are (Figure 2). The addition of GSH, even long after the burst is over, quantitatively converts all RNase to the active form. Thus, at low GSH concentrations, the conversion of misoxidized species to active RNase must be slow. In Scheme I, GSH is shown as participating in the reversal of the formation of misoxidized forms and in their conversion to species that can productively lead to active RNase. The formation of active RNase from the correct PDI substrate is shown as not requiring additional GSSG or GSH, since the observed rate of the fast phase is independent of the GSH and GSSG concentration (Figures 1 and 2).

The actual velocity during the rapid phase of the reaction is comparable to the maximum observed steady-state rate under optimum GSH and GSSG concentrations (Lyles & Gilbert, 1991). The pre-steady-state kinetics are observable not because the rate is particularly fast but because the steady-state rate is slow under these conditions. The overall mechanism shown in Scheme I is consistent with that suggested for the steady-state PDI-catalyzed reaction (Lyles & Gilbert, 1991) and may represent the pre-steady-state behavior of the normal folding pathway(s) under a restricted set of redox conditions.

Disulfide Bond Formation. The formation of disulfide bonds in RNase (Figure 4) is even faster than RNase activation. Within 1 min, the reaction of reduced RNase with GSSG results in the formation of 2 disulfide bond equiv. A typical thiol/disulfide exchange reaction involving normal cysteine residues of pK_a 8.6 occurs with a second-order rate constant of about 150 M^{-1} min^{-1} at pH 8.0 (Gilbert, 1990). With a half-life of less than 0.5 min in the presence of 0.2 mM GSSG, the rapid reaction of GSSG with reduced RNase must occur with a rate constant that is at least 7000 M^{-1} min^{-1}. This is approximately 10–20-fold faster than the appearance of RNase with one disulfide bond observed by Wearne and Creighton (1988) under comparable conditions and may reflect both a statistical effect (RNase has eight cysteines) and the transient accumulation of mixed disulfides between RNase and glutathione. In the absence of PDI, the formation of additional disulfide bonds in RNase is comparable to that expected for freely accessible thiols (k_{obs} = 25 M^{-1} min^{-1}); however, the net oxidation of RNase is accelerated approximately 10-fold (k_{obs} = 2500 M^{-1} min^{-1}) by the presence of 1.4 μM PDI. Thus, PDI is not merely a catalyst for thiol/disulfide rearrangement but it also catalyzes net oxidation of the protein substrate.

Stoichiometric Activation of RNase by PDI. In the presence of sufficient PDI, no thiol/disulfide redox buffer is required to oxidatively activate reduced RNase. The source of the oxidizing equivalents necessary to convert reduced RNase to the native, disulfide form can be provided by PDI itself.

The cDNA sequence of bovine PDI (Yamauchi et al., 1987) indicates the presence of six cysteine residues. Previously (Gilbert, 1989), we reported seven cysteine residues on the basis of sulfhydryl and disulfide titrations; however, one of the seven cysteine residues in the complete cDNA sequence is in the signal sequence and should not be present in mature PDI. However, in the enzyme as isolated, not all of the six cysteine residues are present in disulfide bonds. In 6 M Gdn·HCl, different preparations of PDI show the presence of 0.8–1.3 mol of thiol per mole of PDI and 2.3–2.8 disulfide bonds can be reduced by GSH (Gilbert, 1989). Carmichael et al. (1979) have also detected free cysteine residues in PDI under denaturing conditions. Under nondenaturing conditions, the cysteines are not available for alkylation by iodoacetamide. Alkylation of the free cysteines by NEM does not affect activity, suggesting that the free cysteines are not essential for catalysis (Carmichael et al., 1979).

Four of the six cysteine residues are located in two internally homologous regions of the PDI molecule that have sequence homology to thioredoxin (Edman et al., 1985; Freedman et al., 1988), a small redox active protein that contains two cysteine residues that can exist in either the dithiol or disulfide oxidation states. Hawkins et al. (1986) showed that reduction of PDI followed by the alkylation of two cysteines per mole completely destroyed the activity and suggested that alkylation occurred on one cysteine in each of the two thioredoxin-like domains. On the basis of the observed sequence homology and the recent observation that two of the disulfides are substrates for thioredoxin reductase (Lundstrom & Holmgren, 1990), it is tempting and reasonable to assign these centers to the active site (or sites) of the enzyme.

A titration experiment (Figure 5) demonstrates that 1 mol of reduced RNase requires 1.5 ± 0.2 mol of PDI to restore full activity. Since native RNase has four disulfides per mole, this suggests that PDI must supply 2.6 ± 0.3 disulfide equiv—comparable to its total disulfide content. Thus, at least two, and perhaps all, of the disulfide sites of PDI are kinetically and thermodynamically competent to transfer oxidizing

equivalents into the reduced protein substrate. Consequently, PDI has either multiple active sites or one active site that is capable of delivering the oxidizing equivalents from multiple disulfides.

When PDI is the only source of oxidizing equivalents, the initial rate of RNase regeneration is a complex function of the PDI concentration. Under conditions of reduced RNase excess (low PDI, Figure 6), PDI will be present predominantly in the reduced form, and adding more PDI should simultaneously increase the amount of active enzyme (reduced PDI) and the amount of substrate (oxidized RNase). Thus, the velocity of the reaction would be expected to be proportional to the square of the added PDI concentration. However, rearrangement and redistribution of disulfide bonds among the redox isomers of the RNase substrate and/or PDI itself further complicates the dependence on the PDI concentration.

After a stoichiometric equivalence of PDI has been added, excess PDI inhibits rather than accelerates the oxidative folding of RNase. Clearly, the disulfide form of PDI, which is in molar excess over RNase in the region where inhibition is observed, is not a catalyst of RNase renaturation under these conditions. This suggests that one or more of the reduced forms of PDI are the catalytic species and that the free cysteine residues observed in PDI do not catalyze RNase renaturation. The inhibition observed at high concentrations of PDI could be due to a direct inhibition by PDI binding to itself. Alternatively, the inhibition could result from oxidation of catalytically active PDI by the excess disulfide-containing PDI, which could result in the formation of PDI species with one or two disulfide bonds that are less active than in the fully reduced form of PDI.

At the maximum velocity attained in the absence of a redox buffer, the apparent k_{cat}/K_m for the reaction is approximately 2×10^4 M^{-1} min^{-1}. This is nearly 6-fold slower than the k_{cat}/K_m observed at the optimum GSH and GSSG concentrations for the reaction in a glutathione redox buffer (Lyles & Gilbert, 1991). The actual observed velocity is, however, similar. The 6-fold difference in second-order rate constant arises mainly from the increased concentration of PDI at the point of maximum rate. Limitation of the reaction by factors other than thiol/disulfide exchange, such as proline isomerization (Lang & Schmid, 1988), could account for these results. Alternatively, the glutathione redox buffer could help maintain a more favorable distribution of substrate and/or PDI redox isomers.

PDI is obviously capable of both providing oxidizing equivalents and catalyzing the oxidative folding of RNase. Whether or not this reflects an important property of the in vivo process remains to be determined. However, PDI must be present in very high concentrations in the lumen of the endoplasmic reticulum—approaching millimolar concentrations (Hillson & Freedman, 1984; Lyles & Gilbert, 1991). Regardless of its catalytic role, PDI, because of its high local concentration, must also contribute significantly to the redox buffering capacity of the endoplasmic reticulum.

The ability of PDI to serve as a direct oxidant of RNase and presumably other proteins does not solve the problem of providing oxidizing equivalents to the endoplasmic reticulum. If the oxidant is GSSG, the question of how it gains access to the lumen of the endoplasmic reticulum must be resolved. Ziegler and Poulsen (1977) offered a suggestion in which a ubiquitous flavin monooxygenase situated as an integral membrane protein of the endoplasmic reticulum could provide oxidizing equivalents, originally derived from molecular oxygen, in the form of cystamine $(^+NH_3CH_2CH_2S)_2$. They also showed that this system, in conjunction with added PDI, could significantly accelerate the oxidative folding of reduced RNase (Poulson & Ziegler, 1977).

Registry No. PDI, 37318-49-3; RNase, 9001-99-4; GSSG, 27025-41-8; GSH, 70-18-8.

REFERENCES

Alpert, A. J., & Gilbert, H. F. (1985) *Anal. Biochem. 144*, 553–562.

Bergman, L. W., & Kuehl, W. M. (1979) *J. Biol. Chem. 254*, 8869–8876.

Bulleid, N. J., & Freedman, R. B. (1988) *Nature 335*, 649–651.

Carmichael, D. F., Keefe, M., Pace, M., & Dixon, J. E. (1979) *J. Biol. Chem. 254*, 8386–8390.

Cheng, S., Gong, Q.-H., Parkinson, C., Robinson, E. A., Apella, E., Merlino, G. T., & Pastan, I. (1987) *J. Biol. Chem. 262*, 11221–11227.

Creighton, T. E. (1977) *J. Mol. Biol. 113*, 329–341.

Creighton, T. E. (1978) *Prog. Biophys. Mol. Biol. 33*, 231–298.

Creighton, T. E., Hillson, D. A., & Freedman, R. B. (1980) *J. Mol. Biol. 142*, 43–62.

Creighton, T. E. (1980) *FEBS Lett. 118*, 283–288.

Edman, J. C., Ellis, L., Blacher, R. W., Roth, R. A., & Rutter, W. J. (1985) *Nature 317*, 267–270.

Ellman, G. L. (1959) *Arch. Biochem. Biophys. 82*, 70–77.

Freedman, R. B., Hawkins, H. C., Murant, S. J., & Reid, L. (1988) *Biochem. Soc. Trans. 16*, 96–99.

Geetha-Habib, M., Moiva, R., Kaplan, H. A., & Lennarz, W. J. (1988) *Cell 54*, 1053–1060.

Gilbert, H. F. (1989) *Biochemistry 28*, 7298–7305.

Gilbert, H. F. (1990) *Adv. Enzymol. 63*, 69–172.

Givol, D., Goldberger, R. F., & Anfinsen, C. B. (1964) *J. Biol. Chem. 239*, PC3114–PC3116.

Goldberger, R. F., Epstein, C. J., & Anfinsen, C. B. (1963) *J. Biol. Chem. 238*, 628–635.

Hawkins, H. C., Forster, S. J., Murant, S. J., Wilson, M., & Freedman, R. B. (1986) *Biochem. Soc. Trans. 14*, 756.

Hillson, D. A., Lambert, N., & Freedman, R. B. (1984) *Methods Enzymol. 107*, 281–292.

Koivu, J., Myllyla, R., Helaakoski, T., Pihlajaniemi, T., Tasanen, K., & Kivirikko, K. I. (1987) *J. Biol. Chem. 262*, 6447–6449.

Konishi, Y., Ooi, T., & Scheraga, H. A. (1981) *Biochemistry 20*, 3945–3955.

Konishi, Y., Ooi, T., & Scheraga, H. A. (1982) *Biochemistry 21*, 4734–4740.

Lambert, N., & Freedman, R. B. (1983) *Biochem. J. 213*, 235–243.

Lang, K., & Schmid, F. X. (1988) *Nature 331*, 453–455.

Lundstrom, J., & Holmgren, A. (1990) *J. Biol. Chem. 265*, 9114–9120.

Lyles, M. M., & Gilbert, H. F. (1991) *Biochemistry* (preceding paper in this issue).

Morin, J. E., & Dixon, J. E., (1985) *Methods Enzymol. 113*, 541–547.

Obata, T., Kitagawa, S., Gong, Q.-H., Pastan, I., & Cheng, S.-Y. (1988) *J. Biol. Chem. 263*, 782–785.

Peters, T., & Davidson, L. K. (1982) *J. Biol. Chem. 257*, 8847–8853.

Poulsen, L. L., & Ziegler, D. M. (1977) *Arch. Biochem. Biophys. 183*, 563–570.

Schaffer, S. W., Ahmed, A. K., & Wetlaufer, D. B. (1975) *J. Biol. Chem. 250*, 8483–8486.

Varandani, P. T., Nafz, M. A., & Chandler, M. L. (1975) *Biochemistry 14*, 2115–2120.
Wearne, S. J., & Creighton, T. E. (1988) *Proteins 4*, 251–261.
Wetterau, J. R., Combs, K. A., Spinner, S. N., & Joiner, B. J. (1990) *J. Biol. Chem. 265*, 9800–9807.
Yamauchi, K., Yamamoto, T., Hayashi, H., Koya, S., Takikawa, H., Toyoshima, K., & Horiuchi, R. (1987) *Biochem. Biophys. Res. Commun. 146*, 1485–1492.
Ziegler, D. M., & Poulsen, L. L. (1977) *Trends Biochem. Sci. 2*, 79–81.

Oligosaccharide Structures Present on Asparagine-289 of Recombinant Human Plasminogen Expressed in a Chinese Hamster Ovary Cell Line†

Donald J. Davidson and Francis J. Castellino*
Department of Chemistry and Biochemistry, University of Notre Dame, Notre Dame, Indiana 46556
Received May 10, 1990; Revised Manuscript Received September 21, 1990

ABSTRACT: The oligosaccharide structures linked to Asn^{289} of a recombinant (r) variant ($R^{561}S$) human plasminogen (HPg) expressed in Chinese hamster ovary (CHO) cells, after transfection of these cells with a plasmid containing the cDNA coding for the variant HPg, have been determined. Employing high-performance anion-exchange liquid chromatography mapping of the oligosaccharide units cleaved from the protein by glycopeptidase F, compared with elution positions of standard oligosaccharides, coupled with monosaccharide compositional determinations and analyses of sequential exoglycosidase digestions and specific lectin binding, we find that considerable microheterogeneity in oligosaccharide structure exists at this sole potential N-linked glycosylation site on HPg. A variety of high-mannose structures, as well as bi-, tri-, and tetraantennary complex-type carbohydrate, has been found, in relative amounts of 1–25% of the total oligosaccharides. The complex-type structures contain variable amounts of sialic acid (Sia), ranging from 0 to 5 mol/mol of oligosaccharide in the different glycan structures. Neither hybrid-type moleucles, *N*-acetylglucosamine bisecting oligosaccharides, nor *N*-acetyllactosaminyl-repeat structures were found to be present in the complex-type carbohydrate pool in observable amounts. Of interest, a significant portion of the Sia exists an outer arm structures in an (α2,6) linkage to the penultimate galactose, a novel finding in CHO cell-directed glycosylation. We conclude that considerable differences occur in the N-linked carbohydrate structures of CHO cell-expressed HPg, in insect cell-expressed HPg [Davidson, D. J., Fraser, M. J., & Castellino, F. J. (1990) *Biochemistry 29*, 5584–5590], and in human plasma HPg [Hayes, M. L., & Castellino, F. J. (1979) *J. Biol. Chem. 254*, 8668–8671, 8672–8676, 8677–8680], with both species-specific glycosylation and also protein-directed events of importance in the oligosaccharide trimming and processing that result.

Human plasminogen ([Glu^1]Pg)[1] is the plasma protein zymogen of the enzyme plasmin ([Lys^{78}]Pm), a serine protease with fibrinolytic and fibrinogenolytic properties. [Glu^1]Pg exists in the circulation as a single-chain glycoprotein containing 791 amino acids (Forsgren et al., 1987; Malinowski et al., 1984; McLean et al., 1987; Sottrup-Jensen et al., 1978; Wiman, 1973, 1977) resolvable by affinity chromatography into two major variants (Brockway & Castellino, 1972), which are distinguishable by their respective extents of glycosylation at Asn^{289} (Castellino, 1983; Hayes & Castellino, 1979a–c). One form of the protein contains a biantennary complex oligosaccharide at Asn^{289}, and the other lacks N-linked oligosaccharide (Hayes & Castellino, 1979b), despite the presence of the required consensus tripeptide that directs N-based glycosylation at Asn^{289} (Powell & Castellino, 1983). Both forms of HPg contain O-linked oligosaccharide at Thr^{346} (Hayes & Castellino, 1979c).

We have shown previously that the cDNA for [Glu^1]Pg can be expressed in recombinant baculovirus-infected insect (*Spodoptera frugiperda*) cells (Whitefleet-Smith et al., 1989) and have determined that the Asn^{289}-linked oligosaccharides in the insect-expressed r-[Glu^1]Pg possess some differences from those found in the human plasma protein. In the insect-expressed r-HPg, both complex-type and high-mannose-type oligosaccharide units are present (Davidson et al., 1990a).

The carbohydrate of HPg influences the properties of this zymogen and its corresponding active enzyme. It has been found that HPg form 1 (Asn^{289} is glycosylated) binds differently to lysine-like activation effector molecules (Brockway & Castellino, 1972) and fibrin than HPg form 2 (aglycosyl at Asn^{289}), is activated to HPm at a faster rate (Takada & Takada, 1983), and its corresponding HPm is more rapidly inactivated by its fast-acting plasma-derived inhibitor (Wiman

†Supported by Grant HL-13423 from the National Institutes of Health and the Kleiderer/Pezold Family endowed chair (to F.J.C.).
* To whom correspondence should be addressed.

[1] Abbreviations: CHO, Chinese hamster ovary; HPg and HPm, refer generically to human plasminogen and human plasmin, respectively; [Glu^1]Pg, native human plasminogen with Glu, residue 1, at the amino terminus; [Lys^{78}]Pg, a proteolytically derived form of human plasminogen with Lys, residue 78, at the amino terminus; [Lys^{78}]Pm, human plasmin, which arises from [Glu^1]Pg by cleavage at the activation site, Arg^{561}–Val^{562}, and also at Lys^{77}–Lys^{78}; EACA, ϵ-aminocaproic acid; tPA, tissue plasminogen activator; r, recombinant; wt, wild type; NaDodSO$_4$/PAGE, sodium dodecyl sulfate/polyacrylamide gel electrophoresis; SNA, *Sambucus nigra* agglutinin; WGA, wheat germ agglutinin; NDV, Newcastle disease virus; Gal, galactose; GlcNAc, *N*-acetylglucosamine; Man, mannose; HPLC, high-performance liquid chromatography.

0006-2960/91/0430-625$02.50/0